UCRL-JC-108141
PREPRINT

High-Frequency *P* Wave Spectra from Explosions and Earthquakes

William R. Walter
Keith F. Priestley

This paper was prepared for submittal to the American Geophysical Union
Monograph on Explosion Source Phenomenology
(DOE/LLNL Symposium on Explosion Source Phenomenology,
Lake Tahoe, CA, March 14–16, 1989)

August 6, 1991

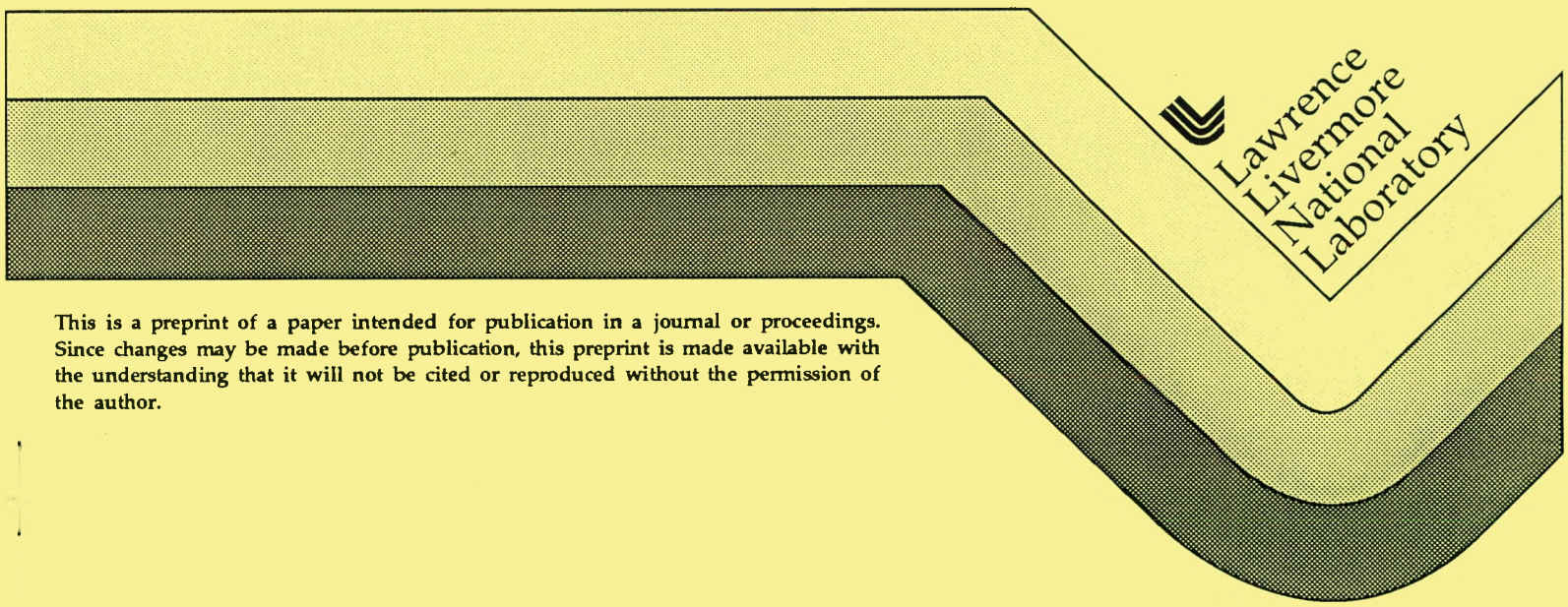

UCRL-JC--108141

DE91 018723

HIGH-FREQUENCY *P* WAVE SPECTRA FROM EXPLOSIONS AND EARTHQUAKES

William R. Walter and Keith F. Priestley[1]

Abstract. Two explosion *P* wave spectral models [Sharpe, 1942; Mueller-Murphy, 1971] and two earthquake *P* wave spectral models [Archambeau, 1968, 1972; modified Brune 1970, 1971] are reviewed to assess their implications for high frequency (>1 Hz) seismic discrimination between earthquakes and explosions. The importance of the corner frequency scaling, particularly for models with the same high frequency spectral decay rate, is demonstrated by calculating source spectral ratios (a potentially important regional discriminant) for these models. We compare North American events and a limited data set of Central Asian events with these spectral models. We find North American earthquakes are consistent with a constant stress drop modified Brune model between 10 and 30 Hz. Shallow (<700 m depth) Pahute Mesa explosions at the Nevada Test Site have a high frequency spectral decay between 10 and 30 Hz greater than the ω^{-2} predicted by the explosion models. Near regional recordings of the Soviet Joint Verification Experiment (JVE) explosion show a higher corner frequency and lower 1 to 4 Hz spectral ratios than predicted by either explosion model. The higher corner frequency of the Soviet JVE appears not to be due to attenuation, or receiver effects, and may represent a need for different corner frequency scaling, or result from source complications such as spall and tectonic release. A regional recording of the Soviet JVE (NEIC m_b = 6.1) is shown to have a lower 1 to 4 Hz spectral ratio than a smaller earthquake (NEIC m_b = 4.6) recorded on a nearly reciprocal path.

Introduction

The United States and the Soviet Union have been observing the terms of the Threshold Test Ban Treaty (TTBT) and the Peaceful Nuclear Explosion Treaty (PNET) since 1976. These treaties limit the maximum yield of underground nuclear testing to 150 kilotons (kt). Large explosions (>20 kt) can be readily detected, and discriminated from earthquakes with seismic waves recorded at teleseismic (>3000 km) distances [cf. Dahlman and Israelson, 1978]. Smaller explosions detonated under these treaties or under a future Comprehensive Test Ban Treaty (CTBT) or lower yield TTBT require detection and discrimination using regional (<3000 km) seismic data. Regional waveforms offer the potential of increased signal bandwidth for detection and identification, particularly at high (>1 Hz) frequencies. Various studies [i.e. Pomeroy et al., 1982; Bennett and Murphy, 1986; and Taylor et al., 1989] suggest that spectral ratios of some regional phases hold promise for discrimination. However, as Taylor et al. [1989] note, ". . . a number of uncertainties regarding the

[1] Seismological Laboratory, Mackay School of Mines, University of Nevada, Reno, Nevada 89557

lack of a physical understanding of how the spectral discriminants work makes their utilization questionable at this point." Under a CTBT or lower yield TTBT there may be a need to detect and identify events from a geographic region in which we have little or no previous experience. In addition it will be necessary to understand under what circumstances a particular detection and identification method might fail. For these reasons it is important to develop a physical understanding of both the source and the propagation characteristics of regional waves.

Separating source and propagation effects can be difficult, particularly for high frequency waves. The observed seismic displacement amplitude spectra $\Omega(\omega)$ can be considered to be the product of a series of linear filters:

$$\Omega(\omega) = S(\omega)\, A(\omega)\, G(\omega)\, I(\omega) \qquad (1)$$

where $S(\omega)$ is the source spectrum, $A(\omega)$ is the attenuation operator, $G(\omega)$ is the Earth's response, $I(\omega)$ is the instrument response, and $\omega = 2\pi f$ is the angular frequency. While $I(\omega)$ is easily determined, any attempt to uniquely isolate $S(\omega)$ is subject to limitations in our knowledge of $A(\omega)$ and $G(\omega)$. The attenuation operator is given as $A(\omega) = e^{\omega t/2Q(\omega)}$ where t is the travel time and $Q(\omega)$ is a dimensionless measure of the energy lost in each seismic wavelength. In most regions $Q(\omega)$ has been found to be a constant or a slowly increasing function of frequency. At higher frequencies the effect of the attenuation operator becomes increasingly important, strongly trading off with estimates of the source spectral amplitude [cf. Anderson, 1986]. Many high frequency (>1 Hz) studies of *P* wave attenuation assume a particular form for the source spectrum and determine the attenuation by adjusting $Q(\omega)$ until the observed spectrum matches the assumed source spectrum [e.g. Der et al., 1985, Hough et al., 1988, Sereno et al., 1988]. The Earth response $G(\omega)$ is also subject to more uncertainty at high frequencies since shorter wavelength signals are affected by small scale features in the Earth. $G(\omega)$ includes source region effects such as free surface reflections, geometrical spreading which may be frequency dependent for some regional phases [e.g. Sereno, 1990], scattering, and receiver site effects. Recent borehole studies at several hardrock sites have found that attenuation and resonance within a shallow weathered zone (typically tens of meters thick) can have a pronounced effect on observed high frequency *P* wave spectra [Malin et al., 1988; L. Carroll, J. Fletcher, H. Liu, and R. Porcella, unpublished data, 1990].

As a result of the difficulties of uniquely determining the source spectral amplitude, various models for both earthquakes and explosions have been proposed, each with different implications for the problems of seismic discrimination. For example, the Sharpe [1942] and Mueller-Murphy [1971] explosion source spectral models are richer in high frequency *P* waves than the Archambeau [1968, 1972] earthquake source spectral model, when normalized to have the same low frequency level. This was the basis for a proposal by Evernden et al. [1986] that the solution to the problem of detection and identification of low-yield underground nuclear explosions was available using high frequency *P* waves. However, if the Brune [1970] earthquake source spectral model

modified for *P* waves [Molnar et al., 1973] is compared with these explosion models the source spectral differences are much smaller.

In this paper we will first review these four competing spectral models and their implications for the seismic discrimination issue, then discuss efforts to distinguish between various earthquake and explosion *P* wave source spectral models using data from western North America. Finally we will compare those results with results from near regional (<800 km) seismic data collected in the vicinity of the Soviet Union's East Kazakhstan Test Site (KTS). Although data for Central Asia is limited, we find significant differences in high frequency (≥1 Hz) *P* wave spectra for Soviet explosions compared with both shallow explosion spectra observed at the Nevada Test Site (NTS) and from explosion spectral models based on North American experience.

Theoretical Models

Simple source spectra are typically characterized by three values: the low frequency asymptote whose level is proportional to the seismic moment (or source strength), the high frequency asymptote whose slope depends on the source displacement time history, and the intersection of these two asymptotes, the corner frequency, f_c, which is related to the source dimension. On a plot of log displacement amplitude versus log frequency the low frequency asymptote has a constant value. The high frequency asymptote is proportional to $\omega^{-\eta}$ where η must be greater than 1.5 to have finite energy. A larger η indicates a greater high frequency decay. Our discussion of spectra for various source models will be in terms of these three parameters.

The generation of seismic waves by an underground nuclear explosion is a complex phenomena. The explosion region can be conceptually modeled with increasing distance from the shot point as a vaporization cavity, a strongly non-linear region characterized by a shock wave, and a linear region [Rodean, 1971]. Sharpe [1942] modeled the seismic waves from explosions as an arbitrary pressure function applied to the interior of a spherical surface at an "elastic radius", R_{el} defined as the distance from the detonation point to the point at which the medium begins to respond linearly (elastically). In the Sharpe model all of the effects of the non-linear region: rock vaporization, cavity expansion, shock wave propagation and decay to an elastic wave, are contained in the form of the pressure function. Sharpe [1942] discussed several pressure histories, but we will follow Evernden et al. [1986], and use a step or Heaviside function in pressure acting at the elastic radius as the "Sharpe" model. The Sharpe far-field displacement amplitude spectrum is given by:

$$\Omega^P(\omega) = \frac{P_o R_{el}^3}{4\mu R}\left(\frac{\alpha^2}{(\alpha^2 - 0.75\, R_{el}^2\omega^2)^2 + (\alpha R_{el}\omega)^2}\right)^{1/2} \qquad (2)$$

where P_o is the amplitude of the pressure step function, μ is the modulus of rigidity, α the *P* wave velocity, and R is the hypocentral distance. Evernden et al. [1986] give a relationship between the elastic radius and the yield as:

$$R_{el} = 1.61 \times 10^4 \left(\frac{kW}{P_o}\right)^{1/3} \text{ meters}, \tag{3}$$

where P_o is in pascals, k is a coupling constant and W is the explosion yield in kilotons. Evernden et al. [1986] give values of P_o = 20 MPa (200 bars), k = 9 for KTS and P_0 = 13 MPa (130 bars), k = 9.4 for NTS.

Mueller and Murphy [1971] modeled explosions with a different pressure function at the elastic radius. They used a pressure function based on free-field observations of several underground nuclear explosions. This pressure function has the form:

$$P(t) = (P_1 e^{-\gamma t} - P_2)\, H(t) \tag{4}$$

where P_1, P_2, and γ are functions of depth and the shot point geology which have been empirically determined from U.S. explosions. The far-field amplitude spectrum of this model is given by:

$$\Omega^P(\omega) = \frac{R_{el}^3}{4\mu R}\left(\frac{P_1^2 + 2P_1P_2}{\gamma^2 + \omega^2} + \frac{P_2^2}{\omega^2}\right)^{1/2} \left(\frac{\alpha^2\omega^2}{(\alpha^2 - 0.75\, R_{el}^2\omega^2)^2 + (\alpha R_{el}\omega)^2}\right)^{1/2}. \tag{5}$$

If we assume a depth–yield scaling relationship appropriate for the NTS of $h = 120\, W^{1/3}$ meters and a granitic medium, then the empirically determined parameters for this model are [Stevens and Day, 1985]:

$$R_{el} \approx 2.38 \times 10^3 \frac{W^{1/3}}{h^{0.42}} \text{ meters}, \tag{6}$$

$$\gamma \approx 1.09 \times 10^4 \frac{1}{R_{el}} \text{ hertz}, \tag{7}$$

$$P_1 \approx 3.77 \times 10^4\, h - P_2 \text{ pascals}, \tag{8}$$

$$P_2 \approx 3.94 \times 10^{14} \frac{W^{0.87}}{R_{el}^3 h^{1/3}} \text{ pascals}. \tag{9}$$

Other models for explosions have been based on fitting polynomials to near-field reduced displacement potentials [Haskell, 1967; von Seggern and Blandford, 1972; Helmberger and Hadley, 1981]. The revision of Haskell's [1967] model proposed by von Seggern and Blandford [1972] gives spectra that are nearly identical to the Mueller-Murphy [1971] model.

The generation of seismic waves by earthquakes has been the subject of many kinematic and dynamic modeling efforts. One the most widely used models of the seismic source spectra is characterized by a single corner frequency and a high frequency decay proportional to ω^{-2} [Aki, 1967; Brune, 1970]. In this paper we examine a specific ω^{-2} model, proposed by Brune [1970], in which the earthquake is modeled as a circular shear crack that slips instantaneously. Here we assume that the *P/S* corner frequency ratio is equal to the *P/S* wave velocity ratio as some studies show [e.g. Molnar, 1973]. The far-field displacement amplitude spectrum for this model is given by [Brune, 1970, 1971]:

$$\Omega^P(\omega) = R_{\Theta\Phi} \frac{r\sigma\alpha}{3R\mu} \frac{1}{\omega^2 + \omega_c{}^2} \tag{10}$$

In (10) σ is the stress drop, r is the radius of the shear crack, $R_{\Theta\Phi}$ is the radiation pattern factor, and ω_c is the angular corner frequency which is given by $\omega_c = 2.34\ \alpha/r$. We will refer to this model as W2P (ω^{-2} decay for *P* waves).

Archambeau [1968, 1972] developed a model for earthquakes in which the seismic waves are generated by the relaxation of pre-existing stress over a spheroidal volume. The high frequency decay for the far-field *P* wave displacement spectrum of this model (with rupture velocity equal or less than the shear wave velocity) is proportional to ω^{-3}. We will refer to this model as W3P. We follow Evernden et al. [1986] in using only the asymptotic values for the far-field spectra of the W3P model. At low frequencies the spectra has a constant low frequency value given by:

$$\Omega_o{}^P = \frac{5\sigma L^3 R_{\Theta\Phi}}{23\mu\alpha R} \tag{11}$$

from zero frequency up to a corner frequency:

$$f_c{}^P = \frac{1}{2\pi L} (3\ \alpha^2 v_r)^{1/3} \tag{12}$$

after which the spectrum decays as ω^{-3}. In equations (11) and (12) L is the maximum rupture dimension and v_r is the rupture velocity. In deriving equation (11) we have assumed a Poisson ratio of 1/4 and set the W3P moment equal to the expression for the zero frequency level of a double-couple point source [Walter et al., 1988].

Making use of equations (2–12) we can compare the high frequency behavior of these models. Figure 1a shows the theoretical far-field amplitude spectra of the Sharpe and Mueller-Murphy (M-M) models calculated for explosions with a yield of 100 kt and 1 kt. For comparison the two earthquake models have also been calculated for the same low frequency values as the Sharpe model. For the W3P model we have assumed that the rupture velocity is equal to the shear wave velocity. This

gives the maximum high frequency values for the W3P model since at higher rupture velocities the spectrum decays as ω^{-2}, and at lower velocities both the corner frequency and spectral amplitudes above the corner frequency decrease [Evernden et al., 1986, Figure 16]. (When the W3P model has rupture velocities slower than the shear wave velocity the asymptotic form of the spectral shape is no longer as good an approximation since the transition between the flat spectrum at low frequencies and the ω^{-3} falloff at high frequencies occurs over a wider frequency band.) Figure 1a shows the large difference in high frequency (>10 Hz) energy content between the W3P and explosion models. Differences between the W2P model and the explosion models are smaller and primarily due to slightly higher corner frequencies of the explosion models.

One of the more promising regional discriminants based on studies of Western U.S. earthquakes and explosions are spectral ratios of regional phases [Murphy and Bennett, 1982; Bennett and Murphy, 1986; Taylor et al., 1988]. The differences in the high frequency falloff between the four models discussed above predict very different source *P* wave spectral ratios. Figure 1b shows the log of the spectral ratio of 1.0 Hz to 4.0 Hz energy as a function of moment, using the same parameters as Figure 1a. For small moments the ratios are unity since both frequencies are on the constant part of the spectrum. For large moments the ratio is a constant value greater than unity, since both frequencies are on the decaying part of the source spectra. For these higher moments the W3P 1.0 to 4.0 Hz ratio is larger than for the other models due to the ω^{-3} decay rate, and suggest the source spectral ratio would be a reliable discriminant between earthquakes and explosions, assuming the W3P and either explosion model is valid. For moments from about 10^{22} to 10^{26} dyne-cm, the frequencies fall on either side of the source corner frequency, and the behavior of the spectral ratio curves in Figure 1b reflect the different corner frequency scaling of each model. If the W2P model for earthquakes is valid, the corner frequency scaling of both the W2P and either explosion model will play a large role in the success of a spectral ratio discriminant based purely on differences in source spectra.

From equations (10–12) we can find a relation for both the W2P and W3P models between low frequency level, stress drop and corner frequency if we hold the medium dependent parameters and observing distance constant:

$$\Omega^P(\omega \to 0) \propto \frac{\sigma}{(f_c^P)^3} \quad . \tag{13}$$

Given two earthquakes with the same moment (i.e. same low frequency level) but different stress drops, the one with the high stress drop has both a higher corner frequency and more high frequency energy than the event with the lower stress drop. A similar relationship can be found for explosions from equations (2) and (5) with the pressure replacing the stress drop:

$$\Omega^P(\omega \rightarrow 0) \propto \frac{P_i}{(f_c^P)^3} \tag{14}$$

where i = 0 for the Sharpe model and i = 2 for the Mueller-Murphy model. For explosions the corner frequency is inversely proportional to the elastic radius [Murphy, 1977]:

$$f_c^P = \frac{\alpha}{2\pi R_{el}} . \tag{15}$$

Equations (13) and (14) show that (for earthquakes and explosions with the same low frequency spectral level) the ratio of explosion corner frequency to earthquake corner frequency depends on the ratio of explosion pressure to earthquake stress drop. For example the Sharpe model with P_o = 200 bars will have about the same corner frequency as W2P model high stress drop earthquakes (100–200 bars). In this case a spectral ratio discriminant will not work very well (see Figure 1b). For extremely high stress drop events (>800 bars), the corner frequencies of the W3P and Sharpe model would be about equal, but the difference in falloff slope should still allow a spectral ratio discriminant to work if one of the frequencies chosen is sufficiently higher than the corner frequency. The Mueller-Murphy pressure P_2 given in equation (9) depends on both yield and depth complicating any simple comparisons. Nevertheless, it is apparent from Figure 1 that in the range from 1 to 100 kt (for the parameters assumed in Figure 1), high stress drop (100–200 bars) W2P earthquakes will not discriminate very well from these Mueller-Murphy explosions on the basis of source spectral ratios.

North American Data

In a previous paper [Walter et al., 1988] we tested some of the specific predictions of the W2P, W3P, and Sharpe models with high sample rate digital data recorded at small hypocentral distances (2–40 km). The earthquake data consist of events from the San Jacinto strike-slip fault region near Anza, California, the subduction zone near Oaxaca, Mexico and the Long Valley caldera and surrounding area near Mammoth Lakes, California. The explosions are NTS explosions from Pahute Mesa. To minimize the effects of attenuation we compared the variation of the earthquake high frequency amplitude with moment for each region using a constant set of stations and events with similar depths and ray paths. The determination of moment based on low frequency spectral amplitudes is relatively insensitive to attenuation and thus any increase in earthquake high frequency spectral amplitude with moment, within each region, can be attributed to a source effect. When comparing the absolute spectral amplitude of explosions with earthquakes, however, we need to take into account attenuation, site, and path effects.

Figure 2a displays 10 Hz *P* wave spectral amplitude as a function of moment for a variety of earthquakes and NTS Pahute Mesa underground nuclear explosions. Theoretical curves have been drawn for the Sharpe explosion model and for the W2P and W3P earthquake models. The

sigmas denote the stress drop in bars for each earthquake curve. In Figure 2a the earthquake 10 Hz amplitudes are consistent with both earthquake models and the explosions show about an order of magnitude scatter near the theoretical Sharpe amplitude prediction. Figure 2b compares 30 Hz *P* wave amplitudes versus moment with the same theoretical curves. The earthquakes show a continued increase in 30 Hz amplitude with moment consistent with an ω^{-2} falloff model and in disagreement with an ω^{-3} model for larger moments.

The explosion spectral amplitudes are from both hardrock and borehole sites (hypocentral distances 15–25 km) and sediment sites (2–12 km). One explosion was recorded on both hardrock and sediment sites; the 10 and 30 Hz spectral amplitudes at the hardrock sites were approximately a factor of two less than at the closer sediment sites. On the basis of limited velocity and attenuation data, Walter et al. [1988] estimated that the sediment recordings should approximate the source spectral amplitude at 10 Hz and underestimate it by about a factor of 3 at 30 Hz. The earthquake amplitudes are all from seismic stations located at hardrock sites (hypocentral distances 5–40 km). Based on estimates of the attenuation at Anza by Hough et al. [1988], we expect the 10 and 30 Hz spectral amplitudes to underestimate the source spectral amplitudes by about a factor of 2 to 3. Site effect studies at Anza show an increase in 10 and 30 Hz spectral amplitude by a factor of about 5 above the free surface effect. Therefore we expect the Anza spectral amplitudes shown in Figures 2a and 2b to slightly overestimate the source spectral amplitudes.

The explosions in Figure 2b separate into two groups: one showing two orders of magnitude less 30 Hz *P* wave energy than predicted by the Sharpe model, the other closer to the Sharpe prediction. The group with less 30 Hz energy was detonated at depths between 600 and 700 m while the group with more 30 Hz energy was detonated at depths of 800 to 1100 m. Thus the shallower group has a high frequency spectral decay between 10 and 30 Hz that is much greater than the ω^{-2} predicted by the Sharpe model. The shallower explosions were detonated near the level of the water table (about 650 m) at Pahute Mesa and we suggested that the location of the explosion relative to the water table may cause the difference in falloff slope between the deep and shallow events [Walter et al., 1988]. These results are similar to the change in high frequency slope observed by Denny [1990] and used by Taylor and Denny [1990] to model spectral differences observed between NTS and KTS explosions. Taylor and Denny [1990] show that for weak porous rock the radiated shock wave divides into a two wave system. In terms of the Sharpe model this is equivalent to introducing a rise time in the pressure function at the elastic radius, so the far-field P spectra then decays as ω^{-3} at high frequencies.

Figures 2a and 2b imply that Anza earthquakes have more 30 Hz *P* wave energy than NTS Pahute Mesa explosions detonated near the water table, in contrast to the Evernden et al. [1986] proposal. Chael [1988] has noted that the slope of the P_g spectra discriminate between NTS explosions and western U.S. earthquakes in the opposite sense of the Evernden et al. [1986] proposal since the explosions had steeper high frequency spectral slopes than the earthquakes. Murphy and Bennett [1982] and Taylor et al. [1988] used low to high frequency spectral ratios for P_n, P_g, and L_g and noted that the NTS explosions had less high frequency energy than the western U.S. earthquakes. In contrast, Taylor and Marshall [1990] compared KTS events to shallow Asian earthquakes and found that the explosions had more high frequency *P* wave energy than the

earthquakes. The material properties and depth to the water table at KTS are very different from NTS. This raises the questions of what are the corner frequency scaling and high frequency decay slope for Soviet KTS explosions, and, whether Soviet explosions can be discriminated from earthquakes in either the manner of Evernden et al. [1986], or the manner of Chael [1988]. We seek a preliminary answer to these questions by examining the regional seismic data recorded in the vicinity of the Soviet East Kazakh Test Site.

Central Asian Data

Soviet JVE. Figure 3 shows the location of the September 14, 1988 Soviet JVE explosion (NEIC $m_b = 6.1$, about 650 m depth) and the four near regional seismograph stations which recorded the event and whose digital seismograms are available to us. The three closest stations, Karkaralinsk (KKL, $\Delta \approx 255$ km), Bayanaul (BAY, $\Delta \approx 255$ km) and Karasu (KSU, $\Delta \approx 160$ km) were installed as part of a cooperative data collection effort between the Natural Resources Defense Council (NRDC) in the U.S. and the Soviet Academy of Sciences (SAS) in the U.S.S.R. [Priestley et al., 1990]. Both short period (1 s) and broadband (15 s free period) high sample rate (200 sample/s) seismographs recorded the Soviet JVE at the NRDC-SAS sites. The seismometers were located in the same vaults as the previous NRDC-SAS cooperative experiment from 1986–1987 [Berger et al., 1987]. All three of these stations are located on similar granitic intrusions of Paleozoic to early Mesozoic age [Leith, 1987]. The seismograph located at Talgar (TLG, $\Delta \approx 740$ km) is a digital seismograph operated by the SAS and has a free period of 1.6 seconds [Priestley et al., 1990] and a flat velocity response to about 15 Hz. TLG is situated on the Northern flanks of the Zaili-Alatau mountains and is sited within Precambrian and lower Paleozoic crystalline rocks.

Seismograms of the Soviet JVE from the vertical short period components at the three NRDC-SAS sites are shown in Figure 4. The KKL seismogram shows an emergent low frequency first arrival followed about three-quarters of a second later by a low amplitude higher frequency arrival. The BAY seismogram shows a single arrival containing high frequencies. The stations KKL and BAY are past the $P_n - P_g$ crossover distance predicted from the Eastern Kazakhstan velocity structure [Antonova et al., 1978; Leith, 1987; Priestley et al., 1988], and we assume the first low amplitude arrival is P_n. The relatively low frequency content of the first KKL P_n arrival is consistent with this arrival being a head wave; however, the relatively high frequency content of the second low amplitude KKL arrival and the BAY P_n arrival are more consistent with their being turning rays. The P_g wavetrain is dominated by the large amplitude dilatational arrival on the vertical and radial components following the P_n arrival by about 1.5 seconds. The dilatational motion of this arrival suggests a supercritical reflection from the Moho. Synthetic reflectivity seismograms computed for the DSS velocity structure [Leith, 1987] agree in both the $P_n - P_mP$ time interval and with the large amplitude and relatively simple shape of P_mP observed at BAY and, particularly, at KKL [Walter and Patton, 1990, Figure 1]. The closest recording of the Soviet JVE was made at KSU within the $P_n - P_g$ crossover distance. Both the short and long period records show a 3 Hz resonance associated with the site [Berger et al., 1988; Priestley et al., 1990]. The filtered KSU trace in Figure 4 shows a large amplitude arrival

following the first arrival by about two seconds, which is consistent with the time for the P_mP arrival at this distance range.

P wave spectra of the Soviet JVE both corrected and uncorrected for attenuation, from data recorded at BAY and KKL are shown in Figure 5. The spectra from KSU are contaminated by the site resonance and are not shown. In order to estimate the effect of any site resonance at KKL we computed the ratio of the surface to borehole (66 m deep) spectral amplitude from the first six seconds of the *P* wave from the $m_b = 4.6$ earthquake of May 26, 1987. The surface to borehole spectral ratio, shown in Figure 6 displays little evidence of any near surface site effect between 1 and 10 Hz, but there is an amplification of the surface spectra of about 2 to 4 in the 10–30 Hz range. Thus we expect site effects at KKL to have little or no effect on the shape of the spectra less then 10 Hz and a small effect on decay rates above 10 Hz. The first arrival of this earthquake was not recorded at BAY but a comparison of the surface and borehole (99 m deep) P coda in the 7.2 to 6.0 km/s group velocity window shows no evidence of surface resonance in the 1 to 6 Hz frequency band where the surface recording has a reasonable signal-to-noise ratio. Thus we do not expect the BAY spectral shape to be strongly effected by site effects between 1 and 6 Hz. The borehole instruments at the NRDC-SAS sites had been removed by the time of the Soviet JVE.

Spectra for an equal length data window prior to the P_n or P_g arrival were computed to indicate the noise level and are also shown in Figure 5. The spectra uncorrected for attenuation, should give a minimum estimate for the source corner frequency and a maximum estimate for the source spectral decay slope. The uncorrected P_n and P_g spectra at BAY give similar corner frequencies of 2.6–4.0 Hz and decay as ω^{-3} at higher frequencies. The uncorrected P_n spectra at KKL does not show a clear corner frequency, perhaps because of the complicated multiple arrival as discussed above. The uncorrected P_g spectrum at KKL has an apparent corner frequency of about 1.5 Hz and decays as $\omega^{-1.6}$ from 2 to about 7 Hz steepening to $\omega^{-3.8}$ from 7 to 25 Hz. The corner frequency determined by the intersection of the $\omega^{-3.8}$ asymptote with the low frequency level is about 3 Hz. To correct the P_n spectra for attenuation we used the results of Sereno [1990] who determined P_n attenuation to be given by $Q(f) = 300f^{0.5}$ by assuming a source spectrum similar to the W2P model for both earthquakes and mine blasts, and fitting spectra from data recorded at the three NRDC-SAS sites. Sereno [1990] notes a frequency independent value of $Q = 1175$ fit the data equally well. To correct the P_g spectra for attenuation we have used the P_gQ of 2000, estimated by Given et al. [1990] to be a minimum value for frequencies above 10 Hz on the basis of chemical blasts recorded at the NRDC stations in Kazakhstan. Given et al. [1990] note that the differing ray paths strongly affect the P_g amplitude so that $Q \geq 2000$ should be regarded as a tenuous estimate. The attenuation corrected BAY P_n, P_g and KKL P_g spectra for the Soviet JVE have about the same corner frequencies as the uncorrected spectra. The high frequency decay slopes of the BAY P_n and P_g spectra decay approximately as $\omega^{-2.2}$ in the range of 5–25 Hz. The KKL P_g spectra decay as $\omega^{-1.4}$ in the range from 1.5–7 Hz and as $\omega^{-3.0}$ in the range from 7–25 Hz.

One of the interesting features of the near regional recordings of the Soviet JVE is the large high frequency SH phases apparent on the transverse components shown on the top of Figure 7. The SH pulse on the BAY transverse component has a frequency of about 1 Hz. These

phases have been modeled as tectonic release by Walter and Patton [1990]. It is often assumed that tectonic release has a negligible contribution at frequencies of 1 Hz or greater, but these seismograms raise questions about whether such assumptions are valid for KTS explosions. The middle three traces in Figure 7 show the BAY broadband vertical, radial and transverse components. The bottom three traces show the same seismograms after bandpass filtering with a center period of five seconds. This filtered traces show Love waves on the transverse component which also implies a significant tectonic release accompanying the explosion.

Comparison of Soviet Earthquakes and Explosion. In order to isolate differences in source spectra from propagation effects, we attempt to minimize the effects of attenuation as much as possible by comparing the spectra of two Soviet explosions with the spectra of two earthquakes recorded over similar, but nearly reversed paths. The two earthquakes (whose location is shown in Figure 3) occurred on July 21, 1986 and May 26, 1987. Both events were m_b = 4.6 (NEIC), and were recorded at KKL. The 1986 event was about 610 km distant (NEIC depth 33 km) and the 1987 event was about 740 km distant (NEIC depth 20 km). The two explosions are denoted by solid stars in Figure 3. The easternmost explosion in Figure 3 is the Soviet JVE; the other explosion is an m_b = 4.9 (NEIC) event which occurred at Degelen on October 18, 1988. Both were recorded at the Soviet Academy of Sciences station Talgar (TLG) near Alma-Ata, about 740 km away.

Figure 8 compares instrument-corrected P_n spectra from each event. For these near reciprocal propagation paths the explosions have a relatively greater high frequency decay compared with the earthquakes. Fitting the log-log spectrum from 5 to 20 Hz with a least squares line we obtain fall off slopes of about $\omega^{-3.5}$ and $\omega^{-4.0}$ from the 1986 and 1987 earthquake, respectively. In contrast the JVE explosion has a larger decay, about $\omega^{-5.0}$ between 5 and 15 Hz. The smaller Degelen explosion shows a similar high frequency decay where the signal is above the noise. The explosions have high apparent corner frequencies, about 5 Hz. The earthquakes do not show a well defined apparent corner frequency but show a gradually larger decay rates with increasing frequency.

Discussion

Since we have only a limited Soviet data set, any conclusions are of necessity, preliminary. The steeper high frequency *P* wave spectral decay observed for the Soviet explosions compared with those observed for Central Asian earthquakes (Figure 8) with nearly reciprocal paths, is similar to that observed for North American earthquakes and explosions [Chael, 1988; Walter et al., 1988]. However, although comparing data along nearly reciprocal paths minimizes attenuation effects related to the propagation path, we have not eliminated effects due to the differences in source depth nor the differences in seismograph site effects. The attenuation corrected near regional JVE spectra show falloff slopes between ω^{-2} and ω^{-3}. If the attenuation correction is valid and Soviet earthquakes falloff as ω^{-2}, then the significant difference in slope observed in the near reciprocal path data between the earthquakes and explosions may be partly due to depth dependent attenuation effects, seismograph site effects at TLG, or some a combination of both.

Recordings of the Soviet JVE show more high frequency energy in the 2 to 5 Hz band than predicted by the Sharpe or Mueller-Murphy models.

Priestley et al. [1990] used the L_g amplitude at the near regional NRDC-SAS stations to estimate a yield of about 120 kt for this event. Sykes and Ekstrom [1989] used a combined $m_b - M_s$ magnitude yield relation to obtain a similar value 113 kt. The corner frequency for the Soviet JVE (assuming a 120 kt yield) predicted by the Sharpe model from equation (3) and (15) is about 1.4 Hz. The apparent corner frequency predicted by the Mueller-Murphy model from equations (9) and (15) for a depth of 650 m is about 0.95 Hz. Because of the peaking near the corner frequency in the Mueller-Murphy model, the intersection of the high and low frequency asymptotes gives a slightly higher value for the corner frequency, about 1.7 Hz. The average corner frequency of the Soviet JVE (using the asymptotic corner frequency for the KKL P_g spectrum, and the BAY P_n and P_g spectra) is about 3 Hz. If we assume that this corner is not due to spall, site effects or tectonic release, then both the Sharpe model and the Mueller-Murphy model would appear to under predict the corner frequency from Soviet explosions. However, the large SH phases on the transverse components suggest that complications to the explosion source, such as spall and tectonic release, may be adding significant high frequency energy to this event. Walter and Patton [1990] used surface wave amplitudes from the NRDC-SAS stations to estimate the tectonic release moment at about one fifth to one tenth that of the explosion. If the tectonic release source spectra resemble the typical earthquake spectra (i.e. flat out to a corner and then decaying) it would be difficult to explain the high *P* wave corner frequencies on this basis. Recent theoretical calculations for spall in a velocity model appropriate for KTS [Barker et al, 1990, McLaughlin et al., 1990] give a peaked spectrum at about 1–4 Hz for the JVE. Synthetic calculations for P_n and P_g by McLaughlin et al. [1990] indicate the spectral amplitude at 1–4 Hz may be dominated by spall. Without near source acceleration data, however, it is difficult to determine whether spall is a significant contributor of 1–4 Hz energy for the Soviet JVE. The smaller explosion shown in Figure 8 presumably contains tectonic release and spall signals that are different from the JVE event, yet they have similar apparent corner frequencies at the TLG station.

The relatively high frequency content of the near regional Soviet JVE spectra can also be seen by comparing 1 to 4 Hz spectral ratios with theoretical calculations. We calculated the ratio of the 0.75–1.25 Hz to 3.0–5.0 Hz energy for the attenuation corrected spectra in Figure 5. The BAY P_n, P_g and KKL P_g regional phases give spectral ratios of 2.2, 2.8, and 5.7, respectively The Mueller-Murphy and Sharpe models predict larger spectral ratios of 6.6 and 8.3, respectively. For comparison the W2P earthquake model gives a spectral ratio of 7.2 (100 bar stress drop) or 12.3 (10 bar stress drop), and the W3P earthquake model gives a spectral ratio of about 64 (for either 100 or 10 bar stress drop), when constrained to have about the same low frequency level as the Soviet JVE. Thus the Soviet JVE also shows both smaller explosion spectral ratios than predicted by theory, and than expected for earthquakes.

We also calculated the same spectral ratios of the spectra of the m_b = 6.1 Soviet JVE recorded at TLG and the m_b = 4.6 earthquake that occurred near the TLG station recorded at KKL using the previously assumed Pn attenuation correction [Sereno, 1990]. Again the explosion has a small spectral ratio of about 0.25, which is much less than the ratio of about 4.2 calculated for the earthquake, even though the earthquake is about 1.5 m_b units smaller. The earthquake spectral ratio value of 4.2 is consistent with a 10 bar stress drop W2P model, but the explosion value is again

much lower than either explosion model predicts. Because the paths are nearly reciprocal the ratio of the two different spectral ratios does not depend upon the specific distance attenuation correction chosen, but it may be influenced by depth dependent attenuation or site effects at TLG as noted above. This may be reflected in the less than one explosion spectral ratio value, indicating that there is some peaking of the TLG spectra near 4 Hz. Such peaked spectra are not observed at the closest stations. Overall these observations give similar results to Taylor and Marshall [1990] who found that KTS explosions gave lower 0.5–1.0 Hz to 2.0–3.0 Hz spectral ratios when compared with shallow Central Asian earthquakes at the United Kingdom teleseismic arrays.

Conclusions

The North American earthquake data presented in this paper are consistent with a constant stress drop W2P model, and have more high frequency energy than shallow NTS explosions at Pahute Mesa which show a spectral decay greater than ω^{-3} above 10 Hz. In contrast the attenuation corrected near regional recordings of the Soviet JVE explosion have a spectral decay between ω^{-2} and ω^{-3} from 10 to 25 Hz. These results are approximately consistent with the hypothesis of Taylor and Denny [1990], who found that spectral ratio data from U.S. explosions could be fit by an explosion model that decays as ω^{-3} at high frequencies, KTS (Shagan River) explosion spectral ratios could be fit with a model that decays as ω^{-2}, and both western U.S. and Central Asian earthquake spectral ratios were consistent with an W2P model. In addition, we found the near regional recordings of the Soviet JVE have a higher corner frequency than predicted by both the Mueller-Murphy model for granite and the Sharpe (using Evernden et al. parameters for KTS) model. This higher corner frequency does not appear to be due to attenuation, path or site effects. The higher corner frequency causes a lower observed explosion 1 to 4 Hz spectral ratio for the Soviet JVE than is predicted by the explosion models. Comparing the Soviet JVE explosion with an earthquake recorded on nearly reciprocal paths we find a similarly low 1 to 4 Hz spectral ratio for the explosion and a higher ratio for the smaller m_b earthquake, which may be partly due to depth dependent attenuation, and site effects at TLG. Whether the higher corner frequency for the Soviet JVE is due to a need for a different explosion scaling relationship at KTS than contained in the models reviewed here, or is due to complications in the simple source models, such as spall and tectonic release, needs to be resolved in order to confidently use a discriminant based on differences between earthquake and explosion spectra.

Acknowledgments. We thank George Randall, Steve Taylor and Bill Peppin for helpful discussions. We thank Mikhail Rozhkov and the Soviet Academy of Sciences for providing the explosion recordings at Talgar. The Soviet JVE data collection effort was supported by a grant from the Natural Resources Defense Council. This research was performed under the auspices of the U.S. Department of Energy by the Lawrence Livermore National Laboratory under contract number W-7405-ENG-48, and was also supported by grants from the Air Force Geophysical Laboratory under contract number F19628-89-K-0022, and the National Science Foundation under contract number EAR8708506. We also thank an anonymous reviewer for comments that improved the manuscript.

References

Aki, K., Scaling law of seismic spectrum, *J. Geophys. Res.*, *72*, 1217-1231, 1967.

Anderson, J. G., Implications of attenuation for studies of the seismic source, in *Earthquake Source Mechanics*, S. Das, J. Boatwright, and C. H. Scholtz, Eds., American Geophysical Union Monograph, *37*, 311-318, 1986.

Antonova, L. V., F. F. Aptikayev, R. I. Kurochkina, I. L. Nersesov, A. V. Nikolayev, A. I. Ruzaykin, Y. N. Sedova, A. V. Sitnikov, F. S. Trergub, L. D. Fedorskaya, and V. I. Khalturin, *Experimental Seismic Investigation of the Earth's Interior*, AS USSR, Institute of Physics of the Earth, Publishing House "Nauka," Moscow, 155 pp, 1978.

Archambeau, C. B., General theory of elastodynamic source fields, *Rev. Geophys.*, *6*, 241-288, 1968.

Archambeau, C. B., The theory of stress wave radiation from explosions in prestressed media, *Geophys. J.*, *29*, 329-366, 1972.

Barker, T. G., S. M. Day, K. L. McLaughlin, B. Shkoller, and J. L. Stevens, *An analysis of the effects of spall on regional and teleseismic waveforms using two-dimensional numerical modeling of underground explosions*, Air Force Geophysical Laboratory Report, GL-TR-90-0126, 1990.

Bennett, T. J., and J. R. Murphy, Analysis of seismic discrimination capabilities using regional data from western United States events, *Bull. Seism. Soc. Am.*, *76*, 1069-1086, 1982.

Berger, J, H. K. Eissler, F. L. Vernon, I. L. Nersesov, M. B. Gokhberg, O. A. Stolyrov, and N. T. Tarasov, Studies of high-frequency seismic noise in Eastern Kazakhstan, *Bull. Seism. Soc. Am.*, *78*, 1744-1758, 1988.

Berger, J., J. N. Brune, P. A. Bodin, J. S. Gomberg, D. M. Carrel, K. F. Priestley, D. E. Chavez, W. R. Walter, C. B. Archambeau, T. B. Cochran, I. L. Nersesov, M. B. Gokhberg, O. A. Stolyrov, S. K. Daragen, N. D. Tarasov, and Y. A. Sutelov, A new US-USSR seismological program, *EOS*, *68*, 110-111, 1987.

Brune, J. N. Tectonic stress and the spectra of seismic shear waves from earthquakes, *J. Geophys. Res.*, *75*, 4997-5009, 1970.

Brune, J. N., Correction, *J. Geophys. Res.*, *76*, 5002, 1971.

Chael, E. P., Spectral Discrimination of NTS Explosions and Earthquakes in the Southwestern United States using High-Frequency Regional Data, *Geophys. Res. Lett.*, *15*, 625-628, 1988.

Dahlman, O., and H. Israelson, *Monitoring Underground Nuclear Explosions*, Elsevier Scientific Publishing Co., Amsterdam, 440 pp., 1977.

Denny, M. D., Free-field data and the seismic source function, this volume, 1990.

Der, Z., T. McElfresh, R. Wagner, and J. Bumetti, Spectral characteristics of P waves from nuclear explosions and yield estimation, *Bull. Seism. Soc. Am.*, *75*, 379-390, 1985.

Evernden, J. F., C. B. Archambeau, and E. Cranswick, An evaluation of seismic decoupling and underground nuclear test monitoring using high-frequency seismic data, *Rev. of Geophys.*, *24*, 143-215, 1986

Given, H., N. T. Tarasov, V. Zhuravlev, F. L. Vernon, J. Berger, and I. L Nersesov, High-frequency seismic observations in Eastern

Kazakhstan, USSR, with emphasis on chemical explosion experiments, *J. Geophys. Res., 95*, 295-307, 1990.

Haskell, N. A., Analytic approximation for the elastic radiation from a contained underground explosion, *J. Geophys. Res., 72*, 2583-2595, 1967.

Helmberger, D. V., and D. M. Hadley, Seismic source functions and attenuation from local and teleseismic observations of the NTS events Jorum and Handley, *Bull. Seism. Soc. Am., 71*, 51-67, 1981.

Hough, S. E., J. G. Anderson, J. Brune, F. Vernon, J. Berger, J. Fletcher, L. Harr, T. Hanks, and L. Baker, Attenuation near Anza, California, *Bull. Seism. Soc. Am., 78*, 672-691, 1988.

Leith, W., *Geology of NRDC seismic stations in eastern Kazakhstan, USSR*, USGS Open-file Report 87-597, 1987.

Malin, P. E., J. A. Waller, R. D. Borcherdt, E. Cranswick, E. G. Jensen, and J. van Schaack, Vertical seismic profiling of Oroville microearthquakes: velocity spectra and particle motion as a function of depth, *Bull. Seism. Soc. Am., 78*, 401-420, 1988.

McLaughlin, K., T. G. Barker, and S. M. Day, *Implications of explosion generated spall models: regional seismic signals*, Air Force Geophysical Laboratory Report, GL-TR-90-0133, 1990.

Molnar, P., B. E. Tucker and J. N. Brune, Corner frequencies of P and S waves and models of earthquake sources, *Bull. Seism. Soc. Am., 63*, 2091-2104, 1973.

Mueller, R. A., and J. R. Murphy, Seismic characteristics of underground nuclear detonations: Part I. seismic spectrum scaling, *Bull. Seism. Soc. Am., 61*, 1675-1692, 1971.

Murphy, J. R., Seismic source functions and magnitude determinations for underground nuclear detonations, *Bull. Seism. Soc. Am., 67*, 135-158, 1977.

Murphy, J. R., and T. J. Bennett, A discrimination analysis of short period regional seismic data recorded at Tonto Forest Observatory, *Bull. Seism. Soc. Am., 72*, 1351-1366, 1986.

Pomeroy, P. W., W. J. Best, and T. V. McEvilly, Test ban treaty verification with regional data—a review, *Bull. Seism. Soc. Am., 72*, S89-S129, 1982.

Priestley, K. P., G. Zandt, and G. Randall, Crustal structure in eastern Kazakh, U.S.S.R. from teleseismic receiver functions, *Geophys. Res. Lett., 15*, 613-616, 1988.

Priestley, K. P., W. R. Walter, V. Martynov, and M. V. Rozhkov, Regional seismic recordings of the Soviet nuclear explosion of the Joint Verification Experiment, *Geophys. Res. Lett., 17*, 179-182, 1990.

Rodean, H. C., *Nuclear Explosion Seismology*, U.S. Atomic Energy Commission, Division of Technical Information, 1971.

Sereno, T., S. Bratt, and T. Bache, Simultaneous inversion of regional wave spectra for attenuation and seismic moment in Scandinavia, *J. Geophys. Res., 93*, 2019-2035, 1988.

Sereno, T. J., Frequency-dependent attenuation in Eastern Kazakhstan and implications for seismic detection thresholds in the Soviet Union, *Bull. Seism. Soc. Am.*, in press, 1990.

Sharpe, J. A., The production of elastic waves by explosions pressures, 1. Theory and empirical field observations, *Geophysics, 7*, 144-154, 1942.

Stevens, J. L., and S. M. Day, The physical basis of m_b:M_S and variable frequency magnitude methods for earthquake/explosion discrimination, *J. Geophys. Res.*, *90*, 3009-3020, 1985.

Sykes, L., and G. Ekstrom, Comparison of seismic and hydrodynamic yield determinations for the Soviet joint verification experiment of 1988, *Proc. Natl. Acad. Sci. USA*, *86*, 3456-3460, 1989.

Taylor, S. R., N. W. Sherman, and M. D. Denny, Spectral discrimination between NTS explosions and western United States earthquakes at regional distances, *Bull. Seism. Soc. Am.*, *78*, 1563-1579, 1988.

Taylor, S. R., M. D. Denny, E. S. Vergino, and R. E. Glaser, Regional discrimination between NTS explosions and western U.S. earthquakes, *Bull. Seism. Soc. Am.*, *79*, 1142- 1176, 1989.

Taylor, S. R. and M. D. Denny, *An analysis of spectral differences between NTS and Shagan River nuclear explosions*, Lawrence Livermore National Laboratory, Livermore, CA, Rep. UCRL-102276, 1990.

Taylor, S. R., and P. D. Marshall, Spectral discrimination between Soviet explosions and earthquakes using U.K. array data, *Geophys. J., in press*, 1990.

von Seggern, D. and R. Blandford, Source time functions and spectra for underground nuclear explosions, *Geophys. J. R. Astr. Soc.*, *31*, 83-97, 1972.

Walter, W. R., J. N. Brune, K. Priestley, and J. Fletcher, Observations of high-frequency P wave earthquake and explosion spectra compared with ω^{-2}, ω^{-3}, and Sharpe source models, *J. Geophys. Res.*, *93*, 6318-6324, 1988.

Walter, W. R. and H. J. Patton, Tectonic release from the Soviet Joint Verification Experiment, *Geophys. Res. Lett. 17*, 1517-1520, 1990.

Figure Captions

Fig. 1. A comparison of the Mueller-Murphy (M-M) and Sharpe explosion models with the W2P and W3P earthquake models. (a) Displacement amplitude spectra of the four models calculated for two different low frequency values. The uppermost explosion curves were calculated for an explosion yield of 100 kt. Lower explosion curves calculated for a yield of 1 kt. The earthquake models were calculated to have the same low frequency levels as the Sharpe curves. (b) 1.0 Hz/4.0 Hz spectral ratio versus moment for the three models. In both figures the explosion models calculated using equations (2) and (5–9) with α = 4.6 km/s. For the Sharpe model P_0 = 200 bars and k = 9, for the M-M model equations (6–9) were used. The earthquake models were calculated using equations (10–12) with α = 6.0 km/s and σ = 100 bars. For (b) a single relation appropriate for the earthquake source parameters was used to calculate the moment from the low frequency level.

Fig. 2. *P* wave displacement spectral observations of earthquakes (solid symbols) and Pahute Mesa underground nuclear explosions plotted as a function of moment and compared with theoretical curves. All symbols and curves normalized to 10 km hypocentral distance. The amplitudes of the theoretical curves have been increased by a factor of two, in approximation of the free surface effect. No attenuation correction has been applied to the data. Events where more than one station recording was used have relatively larger symbol size. Theoretical curves given for constant stress drop denoted by σ in bars. W3P model is given for a constant rupture speed equal to the shear wave velocity. The Sharpe curve was calculated assuming P_0 = 130 bars and k = 9.4, values appropriate for NTS [Evernden et al., 1986]. (a) 10 Hz *P* wave displacement spectral amplitude versus moment. (b) 30 Hz *P* wave displacement spectral amplitude versus moment. [From Walter et al., 1988]

Fig. 3. Map showing locations of Soviet events and stations used in this study. The Soviet explosions are denoted by solid stars and the earthquakes are denoted by solid squares. The September 14, 1988 Soviet JVE event is the easternmost star. The seismic recording stations are denoted by solid triangles and three letter abbreviations.

Fig. 4. Short period vertical seismograms of the Soviet JVE recorded at the four regional seismograph sites shown in Figure 3. The upper part of each section of the figure shows 10 seconds of the *P* wave, the lower portion shows 100 seconds of the whole waveform at KKL, BAY, KSU and 150 seconds at TLG. Two expanded plots of the KSU *P* wave are shown, the upper plot is the original data and the lower trace is the same data after low-pass filtering with a butterworth 4 pole filter with a corner at 1.5 Hz in order to remove the 3 Hz site resonance. [Modified from Priestley et al., 1990]

Fig. 5. Spectra of Soviet JVE recorded at stations (a) BAY and (b) KKL. Windows for each are displayed next to the spectra. Dotted lines indicate the spectra of an equal length window preceding the signal to indicate the noise level. Solid lines are the uncorrected signal spectra and dashed lines have been corrected for attenuation as described in the text. Corner frequency is indicated for both the P_n and P_g phases at BAY and for the P_g phase at KKL.

Fig. 6. Ratio of surface-to-borehole *P* wave spectra of the first six seconds of the May 26, 1987 event (NEIC m_b = 4.6, $\Delta \approx$ 740 km) recorded at KKL. The borehole seismometers were 66 m below the surface. The spectra were smoothed once with a five point running mean prior to computing the ratio.

Fig. 7. Top three traces are the transverse components of the closest recordings of the Soviet JVE. The middle traces are radial and vertical recordings at BAY. The bottom three traces show the three components at BAY low pass filtered at 0.2 Hz. Each trace is self-scaled. The filtered vertical record is approximately four times larger in amplitude than the filtered transverse component. [From Priestley et al., 1990]

Fig. 8. P_n spectra of Soviet JVE recorded at TLG and two earthquakes recorded with nearly reciprocal paths. Window length was six seconds. The top two traces are the September 14, 1988 Soviet JVE explosion and the October 18, 1988 Degelen explosion recorded at TLG. The bottom two traces are a May 26, 1987 earthquake and the July 21, 1986 earthquake recorded at KKL. Earthquake depths are from NEIC, explosion depths are estimates assuming NTS depth scaling. Note the relatively high corner frequency and steep high frequency falloff of the explosion spectra as compared with the earthquake spectra.

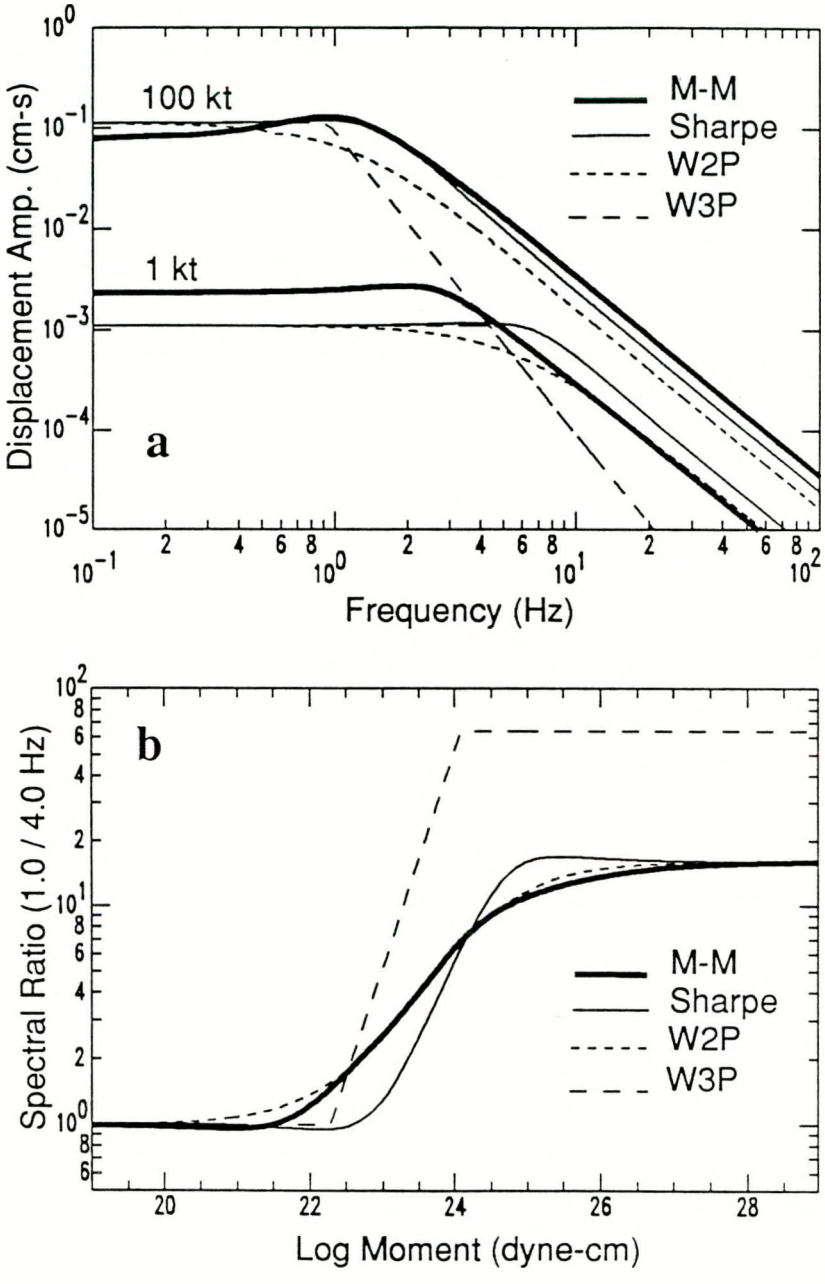
100 kt
1 kt
M-M
Sharpe
W2P
W3P
a
Displacement Amp. (cm-s)
Frequency (Hz)
b
Spectral Ratio (1.0 / 4.0 Hz)
Log Moment (dyne-cm)

Fig. 1

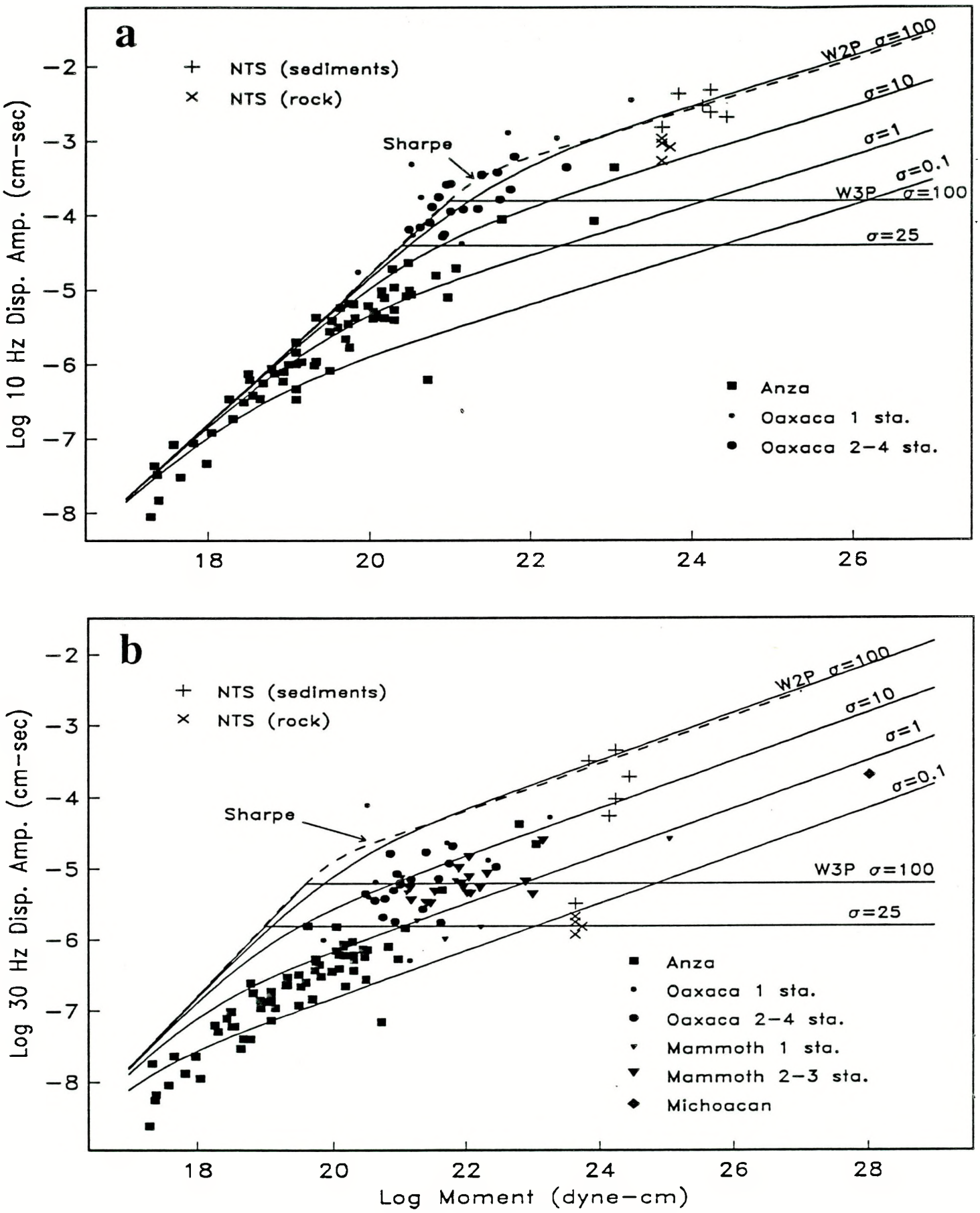
a
NTS (sediments)
NTS (rock)
Sharpe
W2P σ=100
σ=10
σ=1
σ=0.1
W3P σ=100
σ=25
Anza
Oaxaca 1 sta.
Oaxaca 2–4 sta.
Log 10 Hz Disp. Amp. (cm-sec)
−2
−3
−4
−5
−6
−7
−8
18
20
22
24
26
b
NTS (sediments)
NTS (rock)
Sharpe
W2P σ=100
σ=10
σ=1
σ=0.1
W3P σ=100
σ=25
Anza
Oaxaca 1 sta.
Oaxaca 2–4 sta.
Mammoth 1 sta.
Mammoth 2–3 sta.
Michoacan
Log 30 Hz Disp. Amp. (cm-sec)
−2
−3
−4
−5
−6
−7
−8
18
20
22
24
26
28
Log Moment (dyne-cm)

Fig. 2

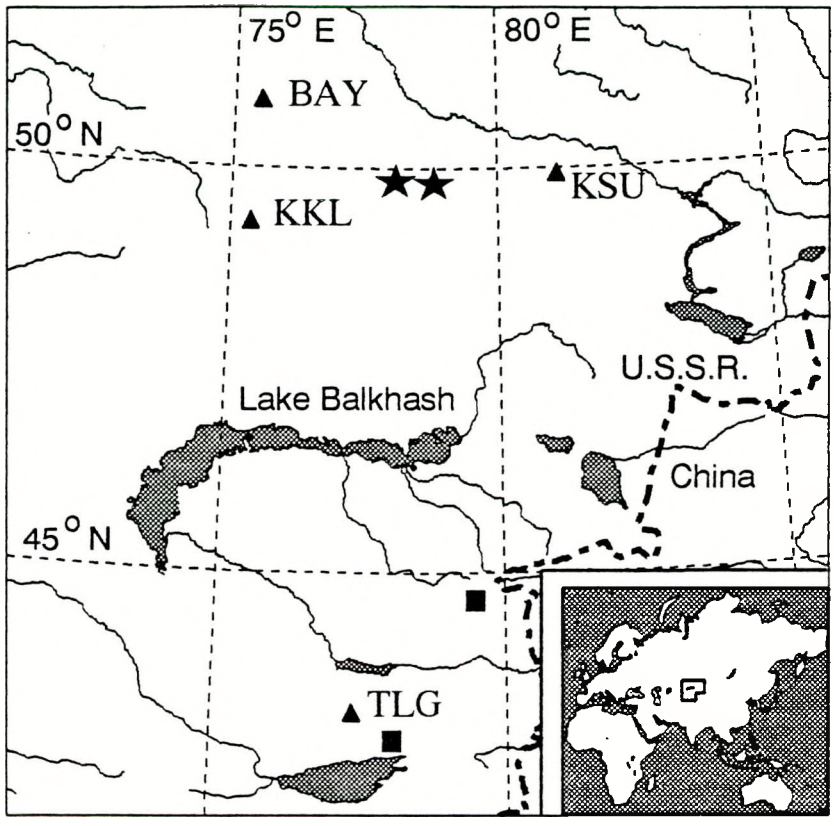

Fig. 3

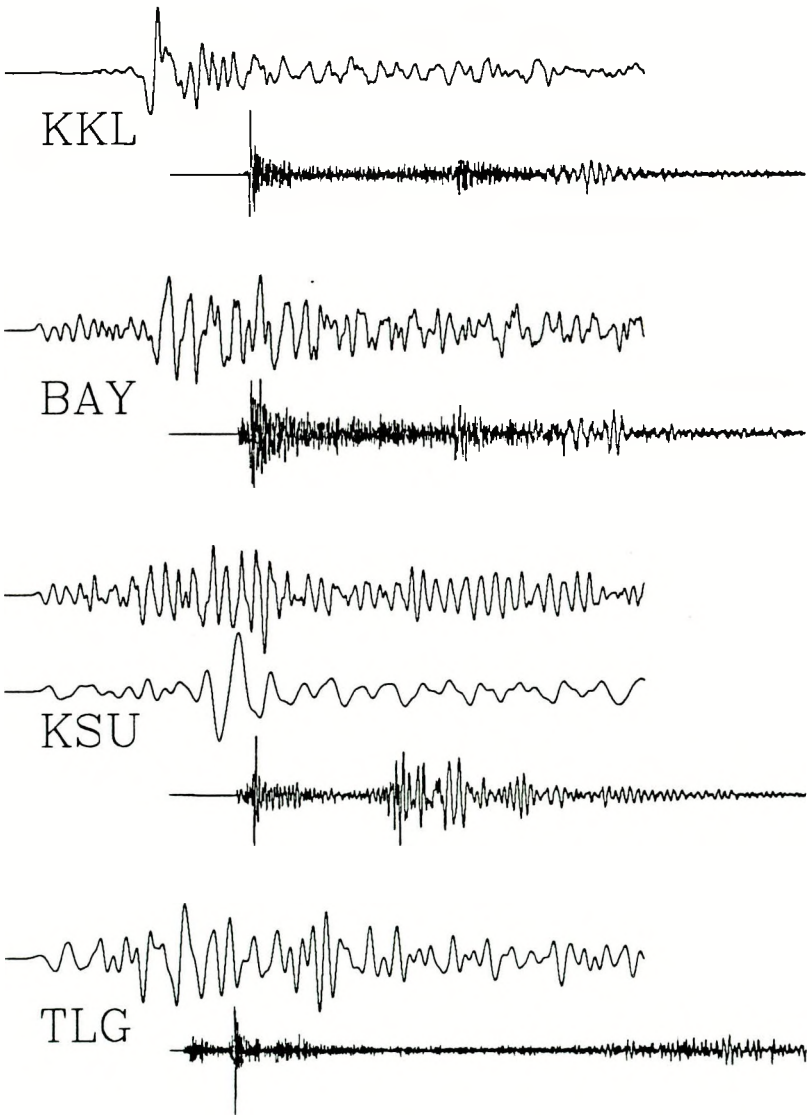

Fig. 4

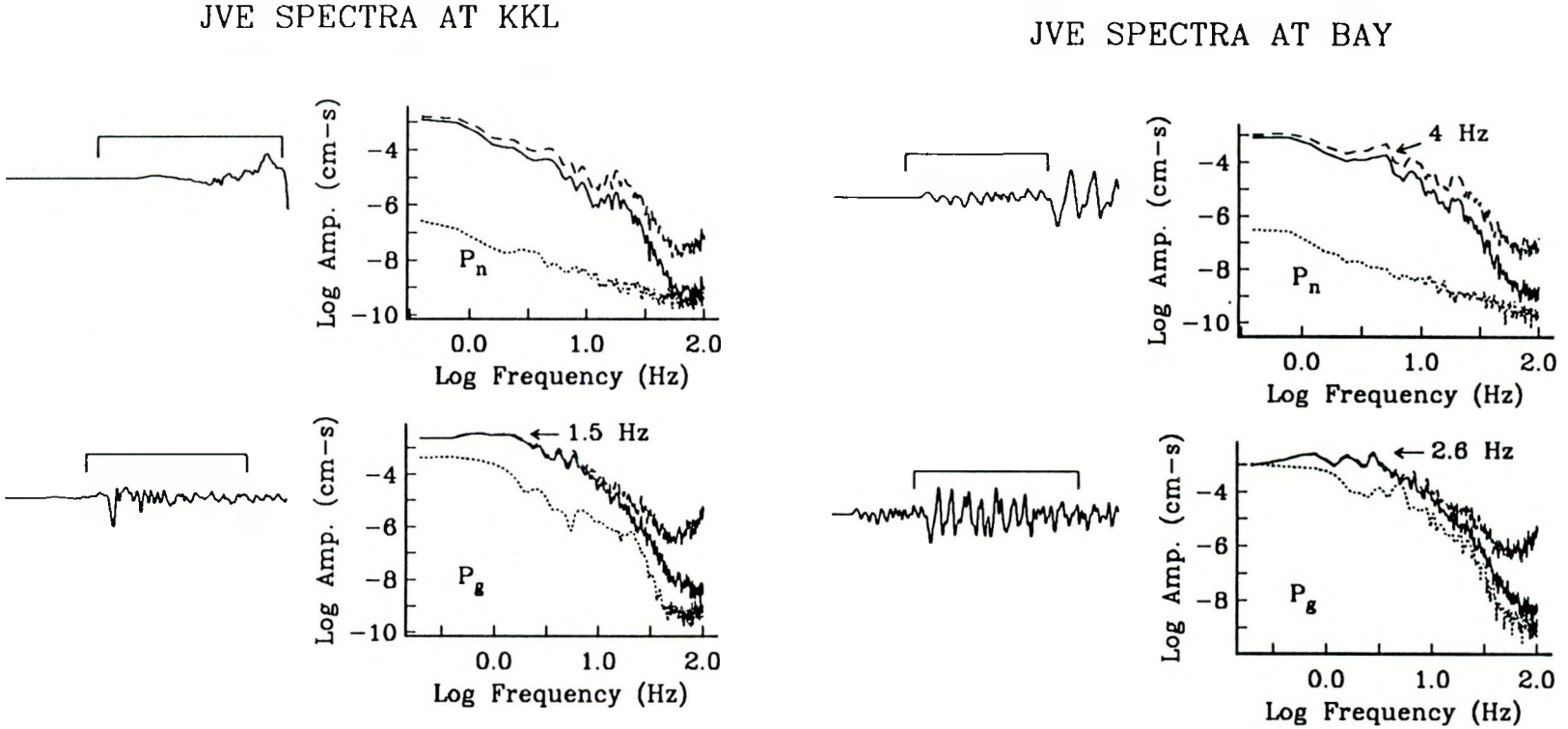
JVE SPECTRA AT KKL
JVE SPECTRA AT BAY
Log Amp. (cm-s)
-4
-6
-8
-10
P_n
4 Hz
0.0
1.0
2.0
Log Frequency (Hz)
1.5 Hz
P_g
2.6 Hz

Fig. 5

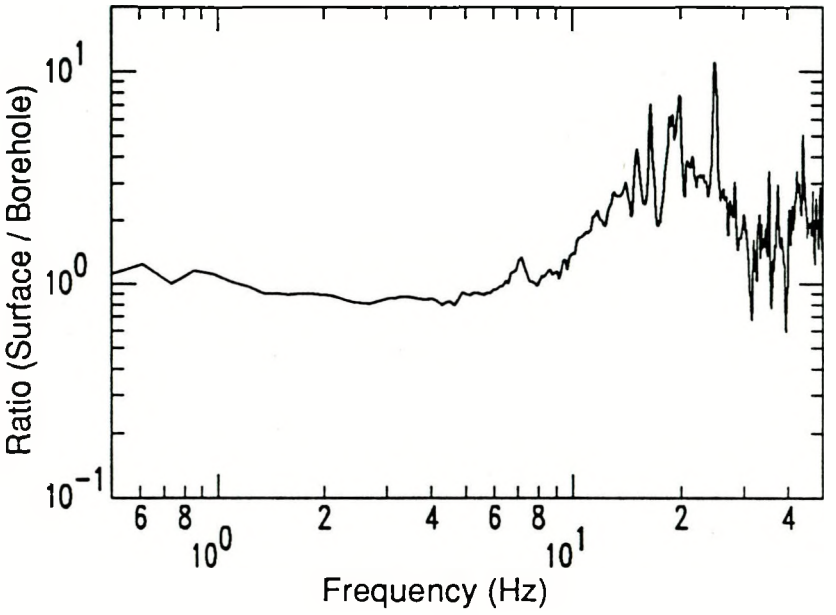
Ratio (Surface / Borehole)
10^1
10^0
10^{-1}
6
8
10^0
2
4
6
8
10^1
2
4
Frequency (Hz)

Fig. 6

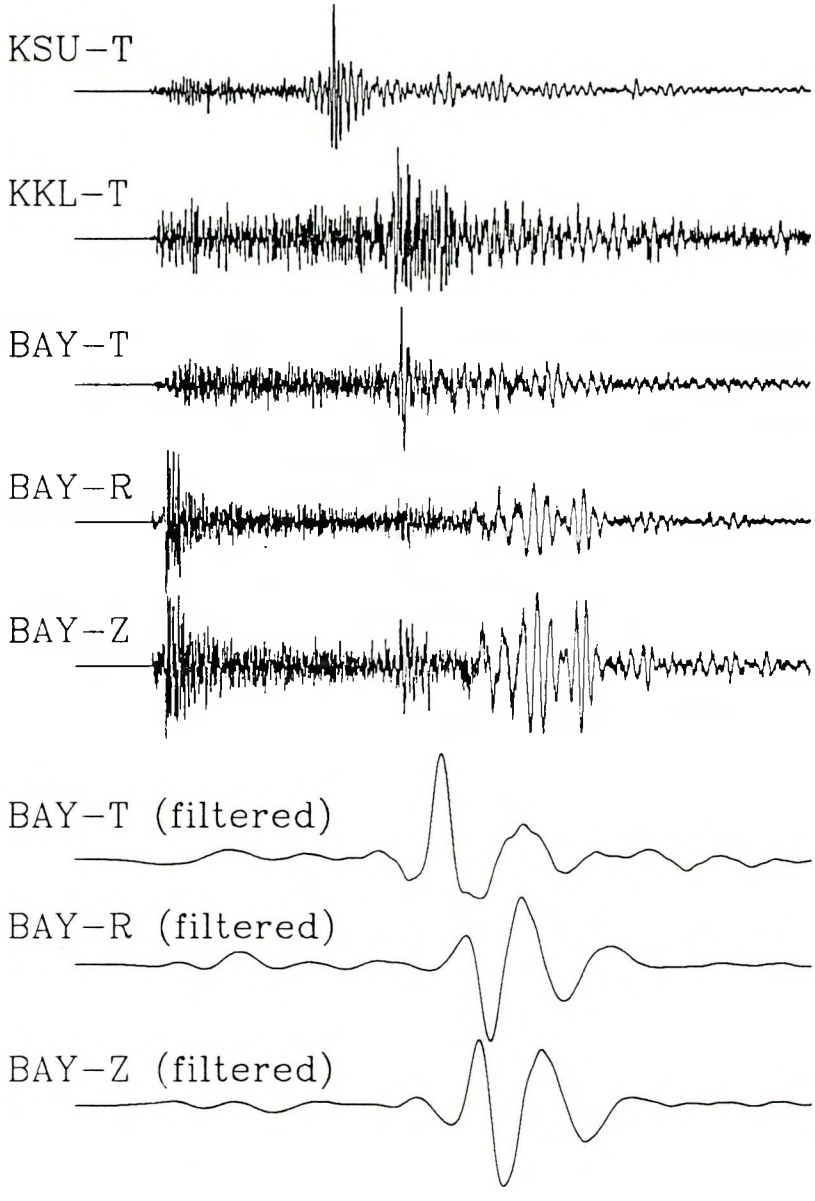
KSU−T
KKL−T
BAY−T
BAY−R
BAY−Z
BAY−T (filtered)
BAY−R (filtered)
BAY−Z (filtered)

Fig. 7

JVE recorded at TLG

(mb=6.1, depth~600 m, Δ=740 km)

Degelen Explosion recorded at TLG

(mb=4.9, depth~300m, Δ=740 km)

Earthquake recorded at KKL

(mb=4.6, depth~33 km, Δ=740 km)

Earthquake recorded at KKL

(mb=4.6, depth~20 km, Δ=610 km)

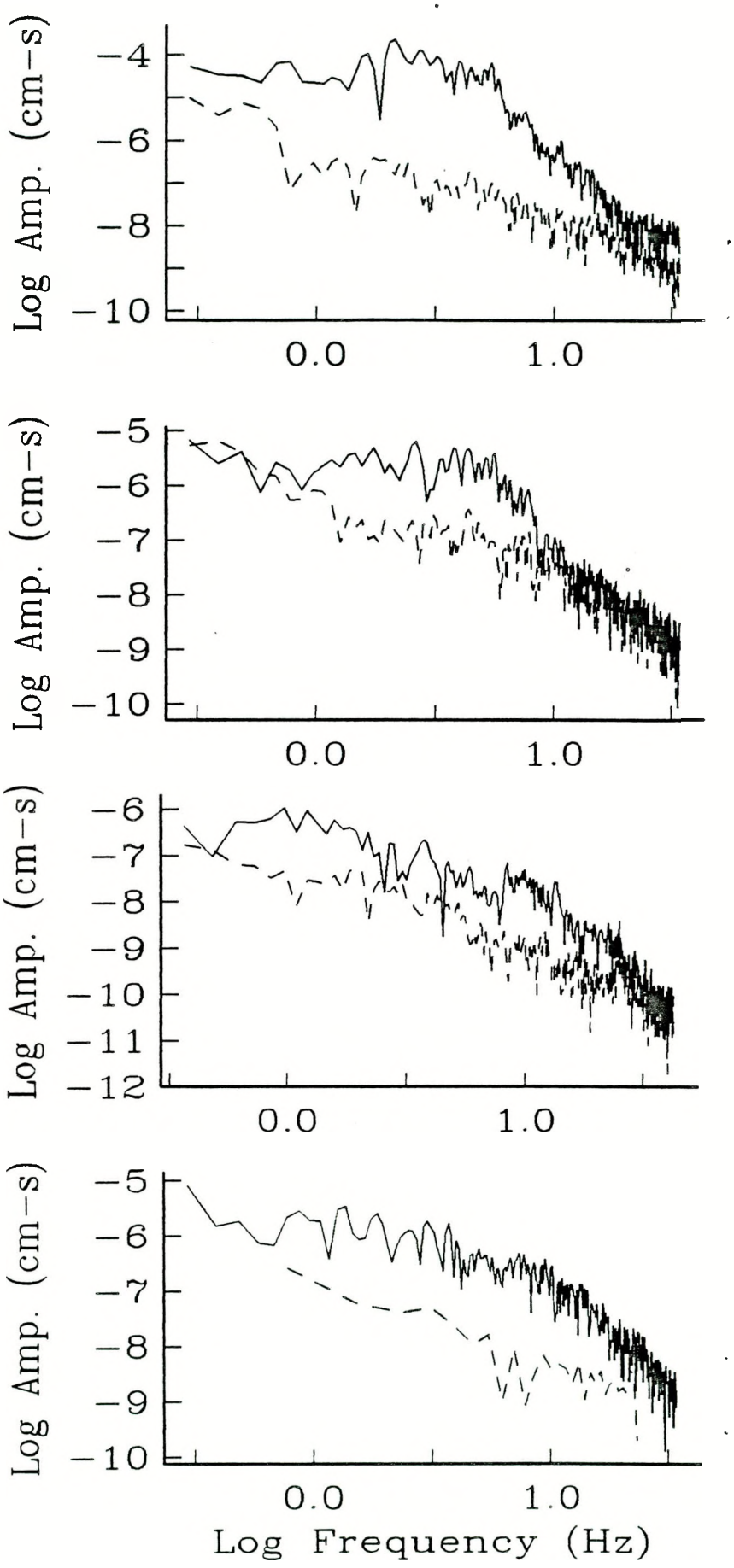

Fig. 8

Technical Information Department · Lawrence Livermore National Laboratory
University of California · Livermore, California 94551